Article

Waste Heat Recovery from Diesel Engine Exhaust Using a Single-Screw Expander Organic Rankine Cycle System: Experimental Investigation of Exergy Destruction

Yeqiang Zhang [1,2,3], **Biao Lei** [4,*], **Zubair Masaud** [5,6], **Muhammad Imran** [7,*], **Yuting Wu** [4], **Jinping Liu** [1], **Xiaoding Qin** [3] and **Hafiz Ali Muhammad** [5,8]

1   School of Electric Power Engineering, South China University of Technology, Guangzhou 510640, China; zhangyeqiang@zzuli.edu.cn (Y.Z.); mpjpliu@scut.edu.cn (J.L.)
2   School of Energy and Power Engineering, Zhengzhou University of Light Industry, No. 5 Dongfeng Road, Zhengzhou 450000, China
3   Guangdong Chigo Air Conditioning Co., Ltd., Foshan 528244, China; jsbqxd@china-chigo.com
4   Key Laboratory of Enhanced Heat Transfer and Energy Conservation, Ministry of Education, Beijing University of Technology, No. 100 Pingleyuan, Chaoyang District, Beijing 100124, China; wuyuting@bjut.edu.cn
5   Korea Institute of Energy Research, Daejeon 305-343, Korea; Zubair@ust.ac.kr (Z.M.); hafiz@kaist.ac.kr (H.A.M.)
6   Department of Advanced Energy and System Engineering, University of Science and Technology, Daejeon 305-350, Korea
7   Mechanical Engineering and Design, College of Engineering and Applied Sciences, Aston University, Birmingham B4 7ET, UK
8   Department of Renewable Energy Engineering, University of Science and Technology, Daejeon 305-350, Korea
*   Correspondence: leibiao@bjut.edu.cn (B.L.); m.imran12@aston.ac.uk (M.I.)

check for updates

Abstract: The organic Rankine cycle is a mature small-scale power generation technology for harnessing low- to mid-temperature heat sources. However, the low efficiency of the cycle still hinders its widespread implementation. To optimize the cycle's performance, it is crucial to identify the source and magnitude of losses within each component of the cycle. This study, thus, aims to investigate the irreversible losses and their effect on the performance of the system. A prototype organic Rankine cycle (ORC) with the exhaust of a diesel engine as the heat source was developed to experimentally investigate the system and ascertain the losses. The experiments were performed at steady-state conditions at different evaporation pressures from 1300 kPa to 1600 kPa. The exergy loss and exergetic efficiency of the individual component and the overall system was estimated from the experimentally measurement of the pressure, temperature, and mass flow rate. The results indicate that the exergy losses of the evaporator are almost 60 kW at different evaporation pressures and the exergy loss rate is from 69.1% to 65.1%, which accounted for most of the total exergy loss rate in the organic Rankine cycle system. Meanwhile, the highest shaft efficiency and exergetic efficiency of the screw expander are 49.8% and 38.4%, respectively, and the exergy losses and exergy loss rate of the pump and pipe are less than 0.5 kW and 1%. Due to the relatively higher exergy loss of the evaporator and the low efficiency of expander, the highest exergetic efficiency of the organic Rankine cycle system is about 10.8%. The study concludes that the maximum improvement potential lies in the evaporator, followed by the expander.

1. Introduction

Internal combustion engines (ICEs) for decades have been the major source of power for locomotives in the world. The stringent local and international limits on the exhaust emission of pollutant gases, such as CO, NOx, CO_2, particulate matter, and other hydrocarbons, have rekindled interest in the development of energy-efficient and cleaner propulsion system for vehicles [1]. Moreover, reduction of the fuel consumption and the amount of greenhouse gases whilst increasing the mechanical performance of ICEs has been the focal point of research in the automotive sector [2]. In ICEs, only about 1/3 of the input fuel energy is converted into useful power [3]; the remainder, amounting to almost 40%, is wasted from the engine exhaust [4]. The harnessing of this enormous waste heat from ICEs can lead to higher efficiencies of the vehicle as well as reductions in global warming [5].

The organic Rankine cycle (ORC) is an established power generation technology for converting low-temperature heat into power. The ORC employs organic working fluids that can be evaporated at considerably low temperatures and can produce work through expansion processes [6]. The ORC system has been widely acknowledged and offers superior performance compared with the incumbent steam or gas cycles for harnessing low-grade heat [7]. Numerous studies investigating the application of ORC in ICEs envisioned that the implementation of ORCs in heavy-duty vehicles has the potential to reduce fuel consumption by 3% to 10% [8]. The ORC is advantageous in terms of affordability, flexibility, adaptability, and low maintenance requirements. Numerous research activities have thermodynamically and experimentally investigated the performance of ORCs integrated with heavy-duty engines [9]. The studies concluded that the need for performance optimization, weight reduction and cost optimization persist for making the system economically viable [10].

The experimental investigation of ORCs for recovering waste heat aimed at studying the operational feasibility of the components while the focus of thermodynamic investigations was to optimize the cycle's performance. Zhang et al. [9] developed a prototype ORC system with a screw expander and compact heat exchangers for the recovery of waste heat from diesel engines. Their experimental results showed the ORC system is compatible with the engine waste heat and can produce 10.38 kW of power with an efficiency of 6.48%. The nature of heat source in ICEs is transient and an improved control strategy is desired for reliable operation. Zhang et al. [11] investigated the control strategy for ORCs in vehicles and designed an improved closed-loop proportional-integral control to regulate the operation. Their results indicated that the proposed control mechanism successfully reduced the response time and improved the output power by 3.23%. Thermodynamic optimization includes the selection of an appropriate ORC working fluid and operating parameters. Bin Wan Ramli et al. [12] studied the potential of ORCs with hybrid vehicles and found out that ORCs can recover 2.02 kW of power from the waste heat with an efficiency of 5.4%. This saving resulted in a 1.2% fuel saving in a standard Worldwide Harmonized Light Vehicle Test Procedure driving cycle test. Bufi et al. [13] performed a comprehensive analysis with various organic working fluids for harnessing waste heat from a diesel engine. They found an optimum combination of operational parameters including evaporation pressure, superheat, and pinch point temperature difference that gave the best performance. Their study showed R11 gives the best efficiency of 20.8% with an evaporation pressure, superheat heat, and pinch point of 3500 kPa, 9.8 K, and 8.5 K, respectively. Yang et al. [14] also performed the optimization of ORCs for engine waste heat with respect to the expander's operating pressure. They showed that at the optimum in and out pressure, the expander can reach up to a maximum power output of 7.13 kW.

Thermodynamic performance assessment provides the optimum operational parameters to maximize the cycle's power output and efficiency. However, the thermodynamically most optimum

cycle configuration does not normally correspond to the most cost-effective solution. Therefore, some researchers resort to the techno-economic analysis of ORC systems. Hajabdollahi et al. [15] performed a techno-economic assessment and optimization of ORC systems for the recovery of waste heat from a 20 kW diesel engine. They used a genetic algorithm for the simultaneous optimization of efficiency and total annual cost. The Pareto form solution suggested that the best performance was achieved with R123 with the maximum efficiency and lowest annual cost. Yang et al. [16] also carried out a techno-economic assessment to minimize the specific investment cost for heat recovery from a marine engine. Their study presented the specific investment for ORC with R1234yf, R152a, R600a, and R245fa was 0.266 W/$, 0.249 W/$, 0.247 W/$, and 0.244 W/$, respectively. In the case of heat recovery from a locomotive engine, the weight and volume of the systems are key factors [7]. To incorporate this, a bottoming ORC attached to a 2 L gasoline engine was investigated from the viewpoint of techno-economics and sizing [17]. The results estimated the optimum value of the specific investment cost, the heat exchangers' area, and the volume coefficient to be 2515 €/kW, 0.48 m^2, and 2.62 MJ/m^3, respectively.

The literature survey above discussed the experimental and theoretical investigations of ORCs on a system level. However, for low-grade or waste heat conversion systems such as in ICEs, the design of the expansion device is highly critical and has a significant impact on the overall system's performance [18]. A thorough literature review on volumetric expanders suggested that a screw expander is most suitable for small systems with a power capacity of less than 50 kWe [19,20]. Wang et al. [21] performed an experimental investigation of a single-screw expander prototype to study its reliability and operability. They generated power of 5 kW with an inlet pressure and temperature of 0.6 kPa and 107 °C, respectively, with air as the working fluid. The screw expanders are considered to be compatible for the power range encountered in ORC systems. Hence, Lei et al. [22] developed an ORC system with a screw expander prototype and carried out experimental investigation. They investigated a new expander structure that eliminated the under-expansion losses and generated a shaft power output of 8.35 kW with an isentropic efficiency of 73%.

The survey suggests that the literature is rich in the performance assessments of ORCs at component and system levels for harnessing waste heat from diesel engines. Various research activities have sought to overcome the complications associated with the ORC such as space limitations, weight, and cost. However, as can be seen from the previous discussion, different research activities set out to optimize the system based on different objectives. The literature lacks a Second Law of Thermodynamics (exergy) analysis and systematic methodology to optimize the ORC system for engine waste heat recovery application. The losses encountered in the volumetric expanders are mostly compared with turbines, yet the studies focused on identifying and quantifying those losses are scarce [20]. Recently, exergy analysis has been rigorously used for the optimization of thermal energy conversion systems [23]. Exergy analysis has been widely used for the optimization of power generation and refrigeration systems [24,25] and for the identification of the origin and source of irreversibility, as well as for quantifying the rate of irreversibility as exergy destruction ($\dot{Ex}_D$). This study therefore performed exergy analysis on an ORC for waste heat recovery from a diesel engine to quantify the thermodynamic losses in the ORC system's components.

The exergy analysis complements the conventional energy analysis by pointing out the source and magnitude of losses and, consequentially, indicating the potential measures that can be taken to improve the system performance. Conventionally, exergy analysis is applied theoretically [25]; however, distinct from previous works, in this study, the effect of the irreversible losses on the performance of the organic Rankine cycle system has been experimentally investigated. A prototype ORC system with the heat source being the exhaust of a 248 kW diesel engine has been established to experimentally ascertain the temperature, pressure, and mass flow rate of the ORC. The experimental values of the state properties are then provided to the exergy model to calculate the $\dot{Ex}_D$ and losses. The appropriate selection of a working fluid is a critical design parameter for ORC systems. Hajabdollahi et al. [15] showed that R123 surpassed the competitive refrigerants for heat recovery from a diesel engine and

this has been selected as the working fluid for the prototype. The expansion machine that converts the thermal energy of the working fluid into useful power is another key parameter in the design of the ORC system. The same authors demonstrated the feasibility of a single-screw expander for R123-based ORC systems. Therefore, this paper also used the single-screw expander shown in Figure 1 for the investigation. The said expander is simple and cost-effective; however, the exergy losses are significant. The experiments were carried out to study the irreversible loss of all the main components and investigate the influence of different operating conditions on the system's performance. With the aid of exergy analysis, the contribution of each individual component to the overall losses is quantified and the exergetic efficiency of the system is reported.
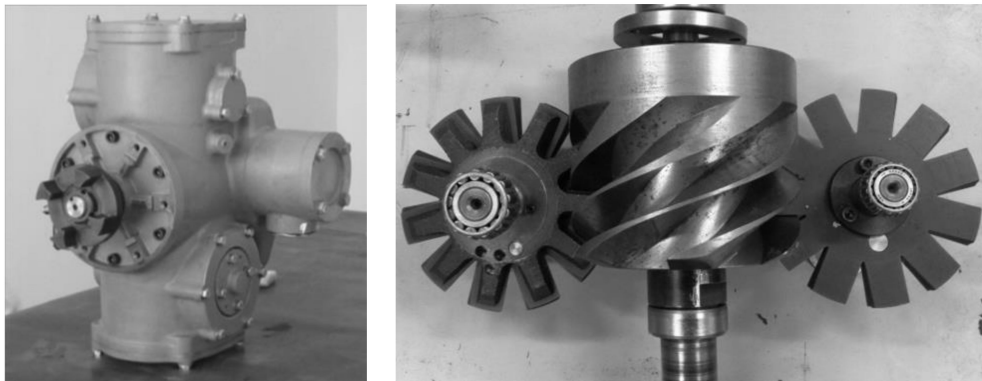
Figure 1. Photo of a single-screw expander. Reprinted with permission. Elsevier, 2020 [9].

Section 2 describes the system and experimental test rig; Section 3 presents the data processing and modeling; Section 4 discusses the insights from the study and the results and discussions; in the end, Section 5 provides the concluding remarks.

## 2. System Description and Test Rig

2.1. System Description

Figure 2 shows the concept of the experimental system and Figure 3 is a photo of the ORC system prototype. In the system, the working fluid is R123 for significantly improving the performance of the system and the heat source is the gas of a diesel engine whose maximum power output is 248 kW. The temperature of the exhaust gas is taken as 485 °C and the engine operating point is kept constant. Although it does not reflect actual engine operation; however, it suffices for the aim of this study, which is to experimentally identify the component with maximum losses and the exergetic efficiency of the cycle. The boundary conditions taken for this analysis are summarized in Table 1.

Table 1. Boundary conditions for the analysis.

Parameters	Values
ORC working fluid	R123
Compressor and turbine isentropic efficiency	0.80
Heat source temperature	485 °C
Maximum heat available	248 kW
ORC evaporation pressure	1300—1600 kPa
Condensing temperature	48.7 ~ 55.4 °C
Reference state (T_o and P_o)	35 °C/101 kPa
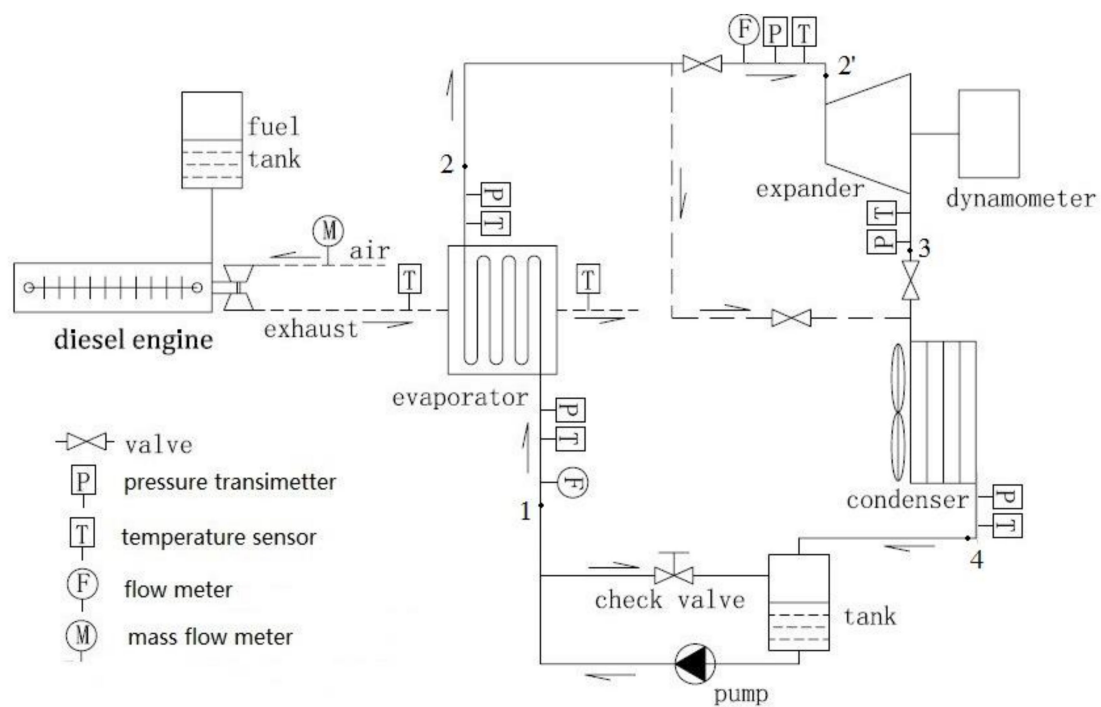
Figure 2. Organic Rankine cycle (ORC) system diagram. Reprinted with permission. Elsevier, 2020 [9].
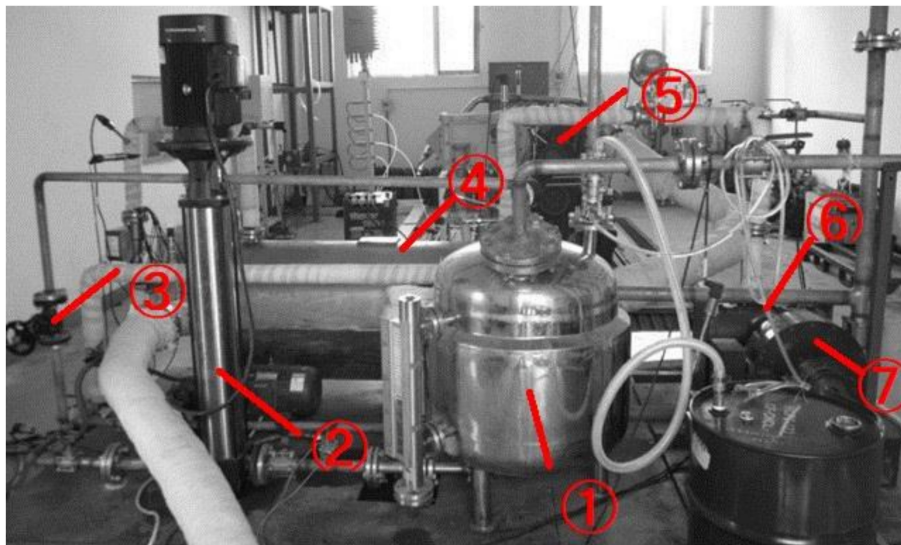
Figure 3. ORC system prototype. 1. Tank; 2. Pump; 3. Check valve; 4. Evaporator; 5. Diesel engine; 6. Expander; 7. Eddy current dynamometer.

In the evaporator, R123 is vaporized under high pressure by absorbing large amounts of heat released from exhaust. Then organic working fluid vapor flows into the single-screw expander and pushes the screw rotation to output work; meanwhile, the pressure of the vapor is decreased until discharged. Before the working fluid is pumped into the evaporator, it is condensed from vapor to liquid in a condenser. The parameters of the components in the system considered in this study are described in paper [11].

2.2. Experimental Test Rig

The geometrical parameters and characteristics of the ORC components are given in Table 2. In order to determine the fluid states at different points, SMP131 pressure transducers and PT100

temperature probes were installed at the points of the evaporator inlet and outlet, the condenser inlet and outlet, and the expander inlet and outlet. Meanwhile, at the evaporator inlet and outlet, N-type temperature probes were installed to measure the temperature of the gas. Between the pump and evaporator, there was a flow meter for measuring the mass flow rates of organic substance; at the inlet of the diesel engine, an air mass flow and an oil consumption meter were installed for calculating the exhaust mass flow rate also. In addition, an eddy current dynamometer was connected by a coupling to a single-screw expander for measuring the rotational speed and calculating the power output. The instrumentation and the propagated uncertainties are listed in Table 3.

Table 2. Characteristics of the components of the ORC system.

Component	Characteristics
Expander	Single-screw expander with CP type Diameter of screw and gaterotor: 155×10^{-3} m Center distance: 124×10^{-3} m Grave number of screws: 6 Tooth number of gaterotor: 11
Evaporator	Shell and tube heat exchanger with spiral titanium tube and baffles Overall dimensions: $\Phi\,500 \times 10^{-3}$ m $\times$ 1500×10^{-3} m Heat exchange area: 12 m^2 Heat input capacity: 152 kW
Condenser	Aluminum multi-channel parallel type condenser with 2 tube sides Overall dimensions: $(980 \times 10^{-3}$ m$) \times (980 \times 10^{-3}$ m$) \times (1255 \times 10^{-3}$ m$)$ Heat transfer area in air side: 90 m^2 Heat rejection capacity: 150 kW
Pump	GRUNDFOS multi-stage centrifugal pump: CR5-32 Designed volume flow: 2.98 m^3/h Designed head: 205 m

Table 3. Instrumentation and propagated uncertainties.

Parameters	Instrument	Accuracy	Full Scale
Temperature	PT100 N-type	±0.5 °C ±1.5 °C	−80 ∼ 300 °C 0 ∼ 800 °C
Pressure	SMP131	±0.5%	0 ∼ 2 MPa
Mass flow rate	Rotameter of H250 Oil consumption meter of FC2210 Thermal gas mass flow meter of 20N150	±1.0% ±0.4% ±1%	25 ∼ 100 L/min 0.1 ∼ 2 kg/min 0 ∼ 2400 kg/h
Torque	GW40 eddy current dynamometer	±0.2%	0 ∼ 160 N × m
Rotational speed	GW40 eddy current dynamometer	±1 rpm	0 ∼ 10,000 rpm

3. Data Processing

At every state, the temperature T and pressure p were measured. Meanwhile, the mass flow $\dot{q}_m$ at different states was equal to the value at the inlet of the evaporator, which was measured by a rotameter. The enthalpy h and entropy s were taken from the property diagram of R123. The exergy analysis grey box model of the ORC system is shown as Figure 4 and the detailed procedure for calculating and applying the exergetic balance is given in Appendix A.
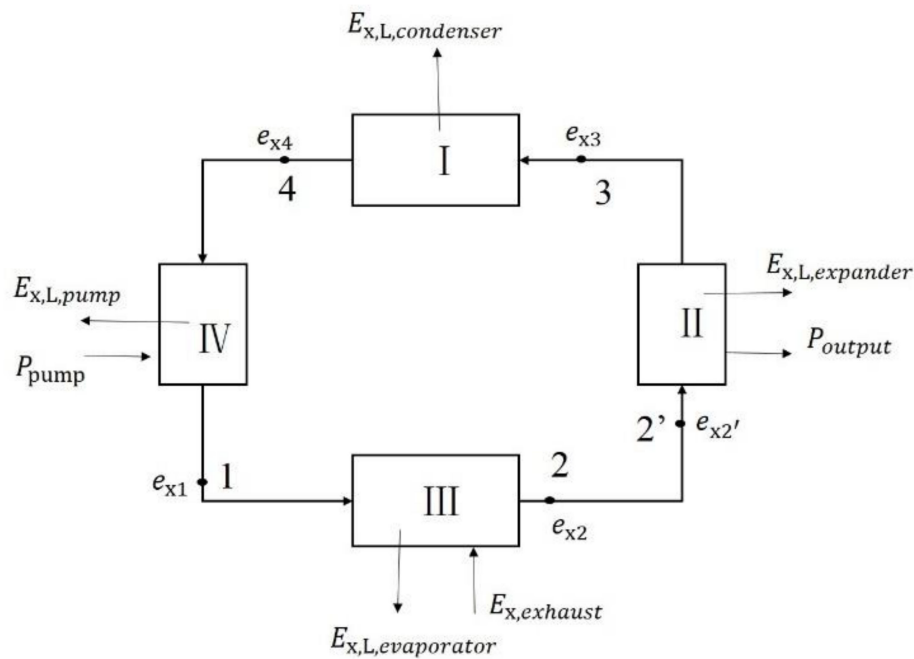
Figure 4. Exergy analysis grey box model of the ORC system.

The η_{Ex} is defined as the ratio of the product and fuel exergy. In an ORC system the output is turbine power (i.e., P_{output}), while the input is P_{pump} and $E\dot{x}_{exhaust}$. Therefore, η_{ex} is defined as in Equation (1):

Exergetic efficiency of the ORC system

$$\eta_{ex,ORC} = \frac{P_{output}}{E\dot{x}_{exhaust} + P_{pump}} \tag{1}$$

4. Results and Discussion

The changes in heat absorbed from exhaust at the evaporator with evaporation pressure are shown as Figure 5. In this figure, the absorption heat from exhaust is from 141.4 kW to 148.9 kW and the difference between the maximum and minimum is not more than 8 kW.
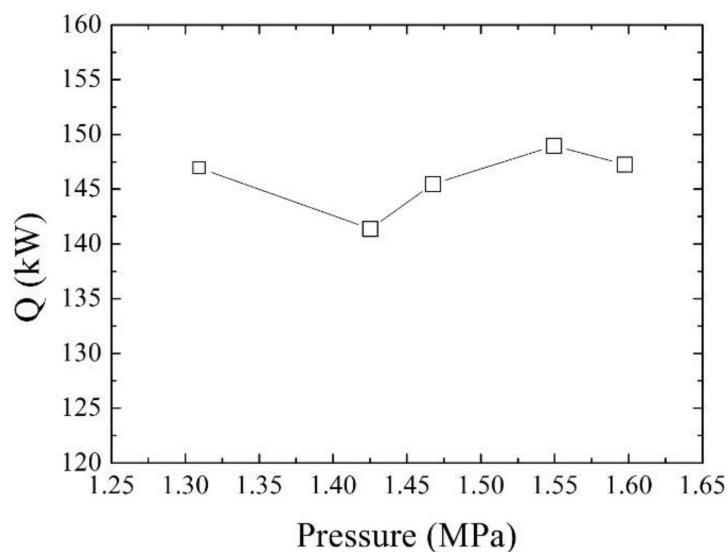
Figure 5. Heat absorbed in the evaporator.

The evolution of temperature in the evaporator during the heat transfer at various pressure values is given in Figure 6. From the figure, it can be seen, due to the location of the pinch point, that the heat transfer process in the evaporator has a lot of irreversibility and therefore high exergy destruction. For the various evaporation pressures, the temperatures of R123 at the inlet/outlet of the evaporator were 39.6/117.1 °C, 42.6/121.9 °C, 45.9/128.9 °C, 48.8/139.6 °C, and 50.4/140.8 °C.
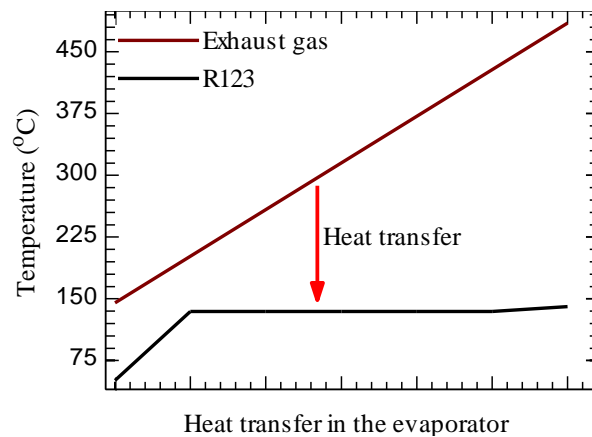

Figure 6. Temperature evolution in the evaporator.

The change in the power output of the expander with evaporator pressure is shown as Figure 7. In this figure, the minimum value is 7.12 kW with 1.31 MPa and the maximum value is 9.62 kW with 1.60 MPa. Due to the increase in evaporation pressure, the expansion ratio across the expander increased, which consequentially led to an increase in power output.
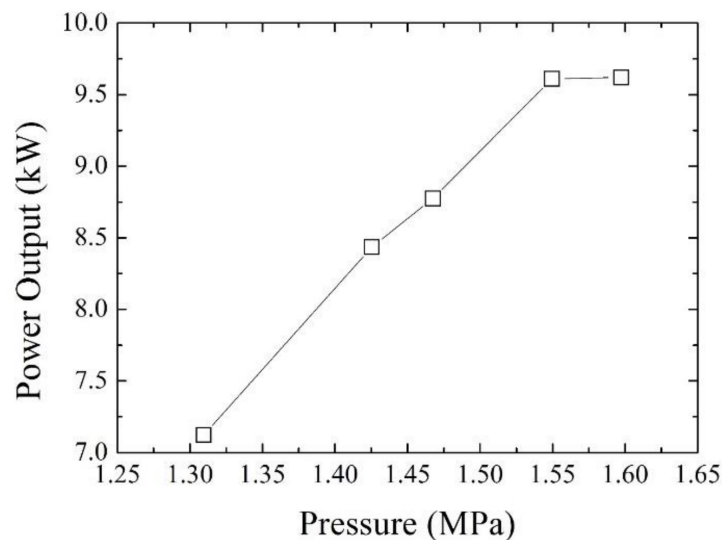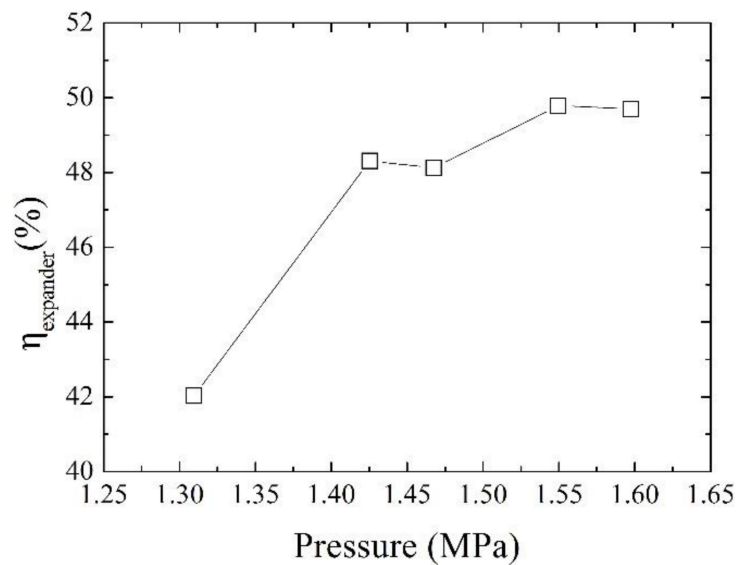

Figure 7. Power output of the single-screw expander.

The change in the shaft efficiency of expander with different evaporator pressures is shown as Figure 8. In the figure, it is shown that the highest value is 49.8% at 1.55 MPa of evaporation pressure and the lowest value is 42.1% at 1.31 MPa of evaporator pressure. Although the shaft efficiency of this expander is increased with the increase in evaporation pressure, it is a little low still and results in lower power output.

Figure 8. Shaft efficiency of the single-screw expander.

The change in the exergy losses of different components with evaporator pressure is shown as Figure 9. In this figure, it is shown that the exergy losses of the evaporator are almost 60 kW at different evaporator pressures, and the values of the expander and condenser are almost 10 kW. Meanwhile, the exergy losses of the pump and pipe can be ignored, as both maximums are less than 0.5 kW.
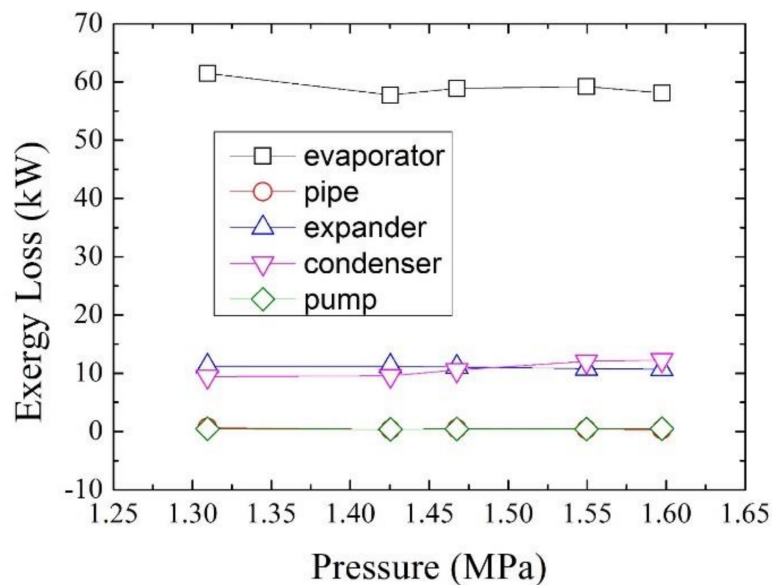

Figure 9. Exergy losses for all components.

Figure 10 shows the changes in the exergy losses rate with evaporation pressure. It is shown that the exergy loss rate occurring in the evaporator accounts for most of the total of the ORC system, which decreased from 69.1% to 65.2% with evaporator pressures from 1.31 MPa to 1.60 MPa. In this figure, the exergy loss rate of the expander is decreased with evaporator pressure and the difference between the highest and the lowest is less than 1.5%, while the values of condenser is increased from 10.6% to 13.8% with the increase in evaporator pressure. In addition, the maximums of the pipe and pump are only 0.74% and 0.55%, respectively.
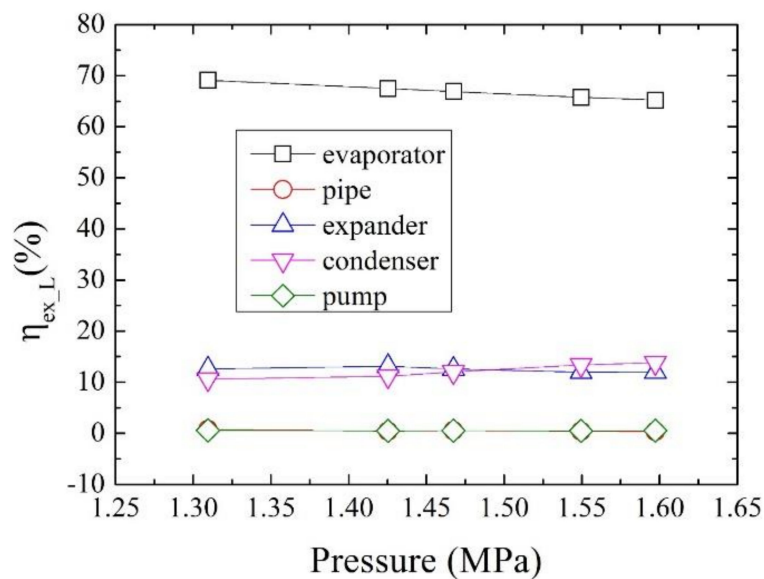
Figure 10. Exergy loss rate of different components.

Figure 11 shows the changes in exergetic efficiency of different components with evaporation pressure. In this figure, it is shown that the exergetic efficiency of the pump is almost 60% but it is 54.0% at an evaporation pressure 1.31 MPa. Meanwhile, the exergetic efficiency of the expander is increased from 32.3% to 38.4% with the increase in evaporation pressure, as well as that of the evaporator increasing from 29.8% to 33.5%. The exergetic efficiency of the condenser and pipe are both 0%, as the exergy released from the condenser and the pipe cannot be used. It is obvious that the decrease in the exergy loss of the evaporator can decrease the exergy loss rate and increase the exergetic efficiency of the evaporator.
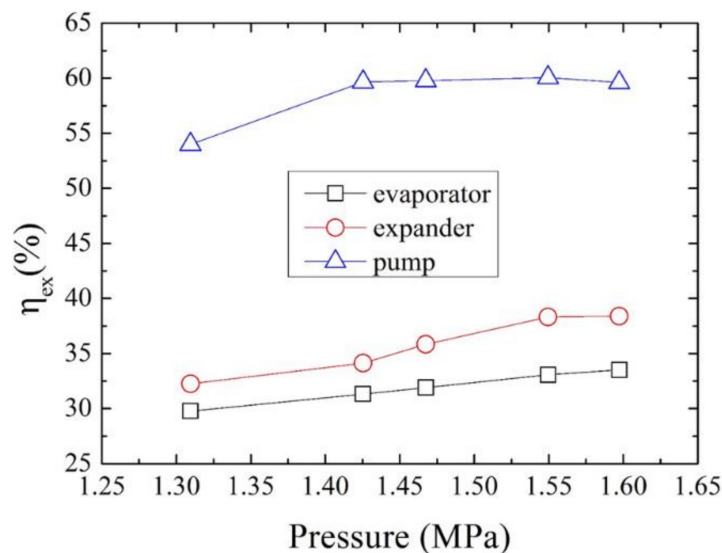
Figure 11. Exergetic efficiency of different components.

Meanwhile, an increase in the single-screw expander's exergetic efficiency can be obtained by increasing its shaft efficiency. Because of the lower exergetic efficiency of the expander and evaporator, the highest exergetic efficiency of the ORC system is 10.8%, which is shown in Figure 12. In this figure, it is shown that the ORC system's exergetic efficiency increased with an evaporation pressure increase from 1.31 MPa to 1.60 MPa.
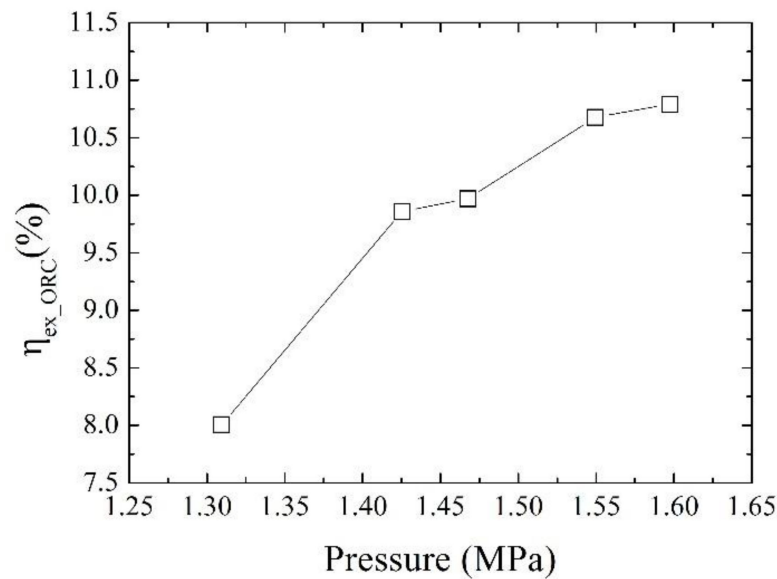
Figure 12. Exergetic efficiency of the ORC system.

Almost all the literature about the exergy performance of ORC systems has been obtained through a mathematical model. These models are always developed for regenerative systems, cascade systems, and series systems. In such systems, a better thermal match is obtained between the source and ORC fluid. Therefore, the exergy performance obtained in this literature is greater than that obtained in this paper. From the insights gained through this study, the next step identified is to analyze the influence of different working fluids on the system's performance including; R245fa, ethanol, zeotropic mixtures, and so on. The performance would be improved by using ethanol or a zeotropic mixture. However, there are many significant problems that need to be solved before using them, such as composition change caused by leakage, which is the subject of further studies.

5. Conclusions

In this study, the effects on the exergy performance indices of different components of an ORC system were investigated and the following results were obtained:

- The exergy losses of the evaporator are almost 60 kW at different evaporation pressures; the corresponding exergy loss rate is from 69.1% to 65.1% and accounts for the most of the total exergy loss rate.
- The expander's maximum shaft efficiency and exergetic efficiency are 49.8% and 38.4%, respectively. Increasing the performance of the expander can increase the power output, and then the system's performance is increased also.
- The exergy losses and exergy loss rate of the pump and pipe are less than 0.5 kW and 1%, respectively, the effects of which on the system's performance can be ignored.

The exergy losses of the evaporator are almost 60 kW at different evaporation pressures, corresponding to exergy loss rates of 69.1% to 65.1% and accounting for the most of the total exergy loss rate. Reducing the average temperature difference between the organic fluid and exhaust is significant for reducing the exergy losses of an evaporator. To achieve this, new organic fluids, especially those that can match the exhaust gas temperature profile better, should be investigated in future.

Appendix A

At every state, the temperature T and pressure p are measured. Meanwhile, the mass flow rate $\dot{q}_m$ at different states is equal to the value at the inlet of the evaporator, which is measured by a rotameter. The enthalpy h and entropy s are taken from the property diagram of R123.

$$h = h(p, T) \tag{A1}$$

$$s = h(p, T) \tag{A2}$$

Then, the exergy (*ex*) and exergy rate $E\dot{x}$ can be calculated as follows:

$$ex = h - h_0 - T_0(s - s_0) \tag{A3}$$

$$E\dot{x} = \dot{q}_m e_x \tag{A4}$$

Appendix A.1. Evaporator

The heat absorbed in the evaporator is Q, and the corresponding exergy is $E\dot{x}_{exhaust}$.

$$Q = \dot{q}_{m,exhaust} c_{p\_exhaust}(T_{exhaust\_in} - T_{exhaust\_out}) \tag{A5}$$

$$E\dot{x}_{exhaust} = Q\left(1 - \frac{T_0}{T}\right) \tag{A6}$$

Meanwhile, the exergy contained in the working fluid entering the evaporator is $e_{x,1}$ and it is $e_{x,2}$ flowing out of the evaporator.

$$e_{x,1} = h_1 - h_0 - T_0(s_1 - s_0) \tag{A7}$$

$$e_{x,2} = h_2 - h_0 - T_0(s_2 - s_0) \tag{A8}$$

Thus, the exergy loss, exergetic efficiency and exergy loss rate are calculated as follows:

$$E\dot{x}_{L,Evaporator} = E\dot{x}_{exhaust} + \dot{q}_{m,R123}(e_{x,1} - e_{x,2}) \tag{A9}$$

$$\eta_{e_x,evaporator} = \frac{\dot{q}_{m,R123}(e_{x,2} - e_{x,1})}{E\dot{x}_{exhaust}} \tag{A10}$$

$$\xi_{evaporator} = \frac{E\dot{x}_{L,Evaporator}}{E\dot{x}_{exhaust} + P_{pump}} \tag{A11}$$

Appendix A.2. Pipe

There are heat losses and pressure losses in the pipe between the evaporator and expander, which cause exergy loss. The exergy loss and exergy loss rate are calculated as follows:

$$e_{x,2'} = h_{2'} - h_0 - T_0(s_{2'} - s_0) \tag{A12}$$

$$Ex_{L,pipe} = \dot{q}_{m,R123}(e_{x,2} - e_{x,2'}) \tag{A13}$$

$$\xi_{pipe} = \frac{Ex_{L,pipe}}{Ex_{exhaust} + P_{pump}} \tag{A14}$$

Appendix A.3. Expander

The power output of the expander is P_{output}, and is also the effective exergy of the output. The exergy loss, exergy loss rate, exergetic efficiency, and shaft efficiency of the expander are calculated as follows:

$$e_{x,3} = h_3 - h_0 - T_0(s_3 - s_0) \tag{A15}$$

$$Ex_{L,Expander} = \dot{q}_{m,R123}(e_{x,2'} - e_{x,3}) - P_{output} \tag{A16}$$

$$\xi_{expander} = \frac{Ex_{L,Evaporator}}{Ex_{exhaust} + P_{pump}} \tag{A17}$$

$$\eta_{ex,expander} = \frac{P_{output}}{\dot{q}_{m,R123}(e_{x,2'} - e_{x,3})} \tag{A18}$$

$$\eta_{expander} = \frac{P_{output}}{\dot{q}_{m,R123}(h_{2'} - h_{3s})} \tag{A19}$$

Appendix A.4. Condenser

The heat released from the condenser cannot be used and thus the reduced exergy cannot be used either, which equals the exergy loss of the condenser. The exergy loss and exergy loss rate are calculated as follows:

$$e_{x,4} = h_4 - h_0 - T_0(s_4 - s_0) \tag{A20}$$

$$Ex_{L,Condenser} = \dot{q}_{m,R123}(e_{x,3} - e_{x,4}) \tag{A21}$$

$$\xi_{condenser} = \frac{Ex_{L,Condenser}}{Ex_{exhaust} + P_{pump}} \tag{A22}$$

Appendix A.5. Pump

The power input of the pump is P_{pump} and the exergy loss, exergetic efficiency, and exergy loss rate are calculated as follows:

$$Ex_{L,Pump} = P_{pump} + \dot{q}_{m,R123}(e_{x,4} - e_{x,1}) \tag{A23}$$

$$\eta_{ex,pump} = \frac{\dot{q}_{m,R123}(e_{x,1} - e_{x,4})}{P_{pump}} \tag{A24}$$

$$\xi_{pump} = \frac{Ex_{L,Pump}}{Ex_{exhaust} + P_{pump}} \tag{A25}$$

References

1. Fatigati, F.; Bartolomeo, M.D.; Battista, D.D.; Cipollone, R. Experimental validation of a new modeling for the design optimization of a sliding vane rotary expander operating in an orc-based power unit. *Energies* **2020**, *13*, 4204. [CrossRef]
2. Bull, J.; Buick, J.M.; Radulovic, J. Heat Exchanger Sizing for Organic Rankine Cycle. *Energies* **2020**, *13*, 3615. [CrossRef]

3.　Domingues, A.; Santos, H.; Costa, M. Analysis of vehicle exhaust waste heat recovery potential using a Rankine cycle. *Energy* **2013**, *49*, 71–85. [CrossRef]

4.　Yu, C.; Chau, K.T. Thermoelectric automotive waste heat energy recovery using maximum power point tracking. *Energy Convers. Manag.* **2009**, *50*, 1506–1512. [CrossRef]

5.　Wang, E.H.; Zhang, H.G.; Fan, B.Y.; Ouyang, M.G.; Zhao, Y.; Mu, Q.H. Study of working fluid selection of organic Rankine cycle (ORC) for engine waste heat recovery. *Energy* **2011**, *36*, 3406–3418. [CrossRef]

6.　Wang, S.; Yuan, Z.A. Hot water split-flow dual-pressure strategy to improve system performance for Organic Rankine Cycle. *Energies* **2020**, *13*, 3345. [CrossRef]

7.　Imran, M.; Haglind, F.; Lemort, V.; Meroni, A. Optimization of organic Rankine cycle power systems for waste heat recovery on heavy-duty vehicles considering the performance, cost, mass and volume of the system. *Energy* **2019**, *180*, 229–241. [CrossRef]

8.　Horst, T.A.; Tegethoff, W.; Eilts, P.; Koehler, J. Prediction of dynamic Rankine Cycle waste heat recovery performance and fuel saving potential in passenger car applications considering interactions with vehicles' energy management. *Energy Convers. Manag.* **2014**, *78*, 438–451. [CrossRef]

9.　Zhang, Y.-Q.; Wu, Y.-T.; Xia, G.-D.; Ma, C.-F.; Ji, W.-N.; Liu, S.-W.; Yang, K.; Yang, F.-B. Development and experimental study on organic Rankine cycle system with single-screw expander for waste heat recovery from exhaust of diesel engine. *Energy* **2014**, *77*, 499–508. [CrossRef]

10.　Shi, L.; Shu, G.; Tian, H.; Deng, S. A review of modified Organic Rankine cycles (ORCs) for internal combustion engine waste heat recovery (ICE-WHR). *Renew. Sustain. Energy Rev.* **2018**, *92*, 95–110. [CrossRef]

11.　Zhang, W.; Wang, E.; Meng, F.; Zhang, F.; Zhao, C. Closed-loop PI control of an Organic Rankine Cycle for engine exhaust heat recovery. *Energies* **2020**, *13*, 3817. [CrossRef]

12.　Bin Wan Ramli, W.R.; Pesyridis, A.; Gohil, D.; Alshammari, F. Organic Rankine Cycle Waste Heat Recovery for Passenger Hybrid Electric Vehicles. *Energies* **2020**, *13*, 4532. [CrossRef]

13.　Bufi, E.A.; Camporeale, S.M.; Cinnella, P. Robust optimization of an Organic Rankine Cycle for heavy duty engine waste heat recovery. *Energy Procedia* **2017**, *129*, 66–73. [CrossRef]

14.　Yang, F.; Cho, H.; Zhang, H.; Zhang, J.; Wu, Y. Artificial neural network (ANN) based prediction and optimization of an organic Rankine cycle (ORC) for diesel engine waste heat recovery. *Energy Convers. Manag.* **2018**, *164*, 15–26. [CrossRef]

15.　Hajabdollahi, Z.; Hajabdollahi, F.; Tehrani, M.; Hajabdollahi, H. Thermo-economic environmental optimization of Organic Rankine Cycle for diesel waste heat recovery. *Energy* **2013**, *63*, 142–151. [CrossRef]

16.　Yang, M.H.; Yeh, R.H. Thermodynamic and economic performances optimization of an organic Rankine cycle system utilizing exhaust gas of a large marine diesel engine. *Appl. Energy* **2015**, *149*, 1–12. [CrossRef]

17.　Galindo, J.; Climent, H.; Dolz, V.; Royo-Pascual, L. Multi-objective optimization of a bottoming Organic Rankine Cycle (ORC) of gasoline engine using swash-plate expander. *Energy Convers. Manag.* **2016**, *126*, 1054–1065. [CrossRef]

18.　Wronski, J.; Imran, M.; Skovrup, M.J.; Haglind, F. Experimental and numerical analysis of a reciprocating piston expander with variable valve timing for small-scale organic Rankine cycle power systems. *Appl. Energy* **2019**, *247*, 403–416. [CrossRef]

19.　Imran, M.; Usman, M.; Park, B.-S.; Lee, D.-H. Volumetric expanders for low grade heat and waste heat recovery applications. *Renew. Sustain. Energy Rev.* **2016**, *57*, 1090–1109. [CrossRef]

20.　Imran, M.; Usman, M. Mathematical modelling for positive displacement expanders. In *Positive Displacement Machines*; Academic Press: New York, NY, USA, 2019; pp. 293–343.

21.　Wang, W.; Wu, Y.-T.; Ma, C.-F.; Liu, L.-D.; Yu, L. Preliminary experimental study of single screw expander prototype. *Appl. Therm. Eng.* **2011**, *31*, 18–88. [CrossRef]

22.　Lei, B.; Wang, W.; Wu, Y.-T.; Ma, C.-F.; Wang, J.-F.; Zhang, L.; Li, C.; Zhao, Y.-K.; Zhi, R.-P. Development and experimental study on a single screw expander integrated into an Organic Rankine Cycle. *Energy* **2016**, *116*, 43–52. [CrossRef]

23.　Muhammad, H.A.; Lee, B.; Sultan, H.; Imran, M.; Baik, Y.-J. Advance thermodynamic analysis of a CO_2 compression system using heat-pump for CCS. In Proceedings of the ECOS 2020—33rd International Conference on Efficiency, Cost, Optimization, Simulation and Environmental Impact of Energy Systems, Osaka, Japan, 29 June–3 July 2020; Available online: https://publications.aston.ac.uk/id/eprint/41661/1/Conference_paper_2.pdf (accessed on 1 September 2020).

24. Lazzaretto, A.; Tsatsaronis, G. SPECO: A systematic and general methodology for calculating efficiencies and costs in thermal systems. *Energy* **2006**, *31*, 9–89. [CrossRef]

25. Ahamed, J.U.; Saidur, R.; Masjuki, H.H. A review on exergy analysis of vapor compression refrigeration system. *Renew. Sustain. Energy Rev.* **2011**, *15*, 1593–1600. [CrossRef]

Publisher's Note: MDPI stays neutral with regard to jurisdictional claims in published maps and institutional affiliations.